

Unsteady effects on natural convective heat transfer through porous media in cavity due to top surface partial convection

W. Pakdee, P. Rattanadecho *

*Department of Mechanical Engineering, Faculty of Engineering, Thammasat University, Rangsit Campus,
Klong Luang, Pathumtani 12120, Thailand*

Received 2 December 2005; accepted 10 March 2006
Available online 24 April 2006

Abstract

Numerical investigations of transient natural convection flow through a fluid-saturated porous medium in a rectangular cavity with a convection surface condition were conducted. Physical problem consists of a rectangular cavity filled with porous medium. The cavity is insulated except the top wall that is partially exposed to an outside ambient. The exposed surface allows convective transport through the porous medium, generating a thermal stratification and flow circulations. The formulation of differential equations is non-dimensionalized and then solved numerically under appropriate initial and boundary conditions using the finite difference method. The finite different equation handling the boundary condition of the open top surface is derived. The two-dimensional flow is characterized mainly by two symmetrical vortices driven by the effect of buoyancy. A lateral temperature gradient in the region close to the top wall induces the buoyancy force under an unstable condition. Unsteady effects of associated parameters were examined. It was found that the heat transfer coefficient, Rayleigh number and Darcy number considerably influenced characteristics of flow and heat transfer mechanisms. Furthermore, the flow pattern is found to have a local effect on the heat convection rate.

© 2006 Elsevier Ltd. All rights reserved.

Keywords: Natural convection; Saturated porous media; Convection boundary condition

1. Introduction

The heat and fluid flows in cavity that experiences convective heating or cooling at the surface are found in a wide variety of applications including lakes and geothermal reservoirs, underground water flow, solar collector etc. [1]. Associated industrial applications include secondary and tertiary oil recovery, growth of crystals [2], heating and drying process [3–5], solidification of casting, sterilization etc.

Natural or free convection in a porous medium has been studied extensively. Cheng [6] provides a comprehensive review of the literature on free convection in fluid-saturated porous media with a focus on geothermal

systems. Oosthuizen and Patrick [7] performed numerical studies of natural convection in an inclined square enclosure with part of one wall heated to a uniform temperature and with the opposite wall uniformly cooled to a lower temperature and with the remaining wall portions. The enclosure is partially filled with a fluid and partly filled with a porous medium, which is saturated with the same fluid. The main results considered were the mean heat transfer rate across the enclosure.

Nithiarasu et al. [8] examined effects of variable porosity on convective flow patterns inside a porous cavity. The flow is triggered by sustaining a temperature gradient between isothermal lateral walls. The variation in porosity significantly affects natural flow convective pattern. Khanafar and Chankha [9] performed numerical study of mixed convection flow in a lid-driven cavity filled with a fluid-saturated porous media. In this study, the influences of the Richardson number, Darcy number and the

* Corresponding author.

E-mail address: ratphadu@engr.tu.ac.th (P. Rattanadecho).

Nomenclature

c_p	specific heat capacity (J/kg K)	β	coefficient of thermal expansion (1/K)
Da	Darcy number (–)	ε	porosity (–)
g	gravitational constant (m/s ²)	μ	dynamic viscosity (Pa/s)
H	cavity length (m)	ν	kinematics viscosity (m ² /s)
h	convective heat transfer coefficient (W/m ² K)	ρ_f	fluid density (kg/m ³)
k	effective thermal conductivity of the porous medium (W/m K)	τ	dimensionless time
p	pressure (Pa)	θ	dimensionless temperature
Pr	Prandtl number (–)	ω	vorticity (m ² /s)
Ra	Rayleigh number (–)	ψ	stream function
T	temperature (°C)	ζ	dimensionless vorticity
t	time (s)	Ψ	dimensionless stream function
u, v	velocity component (m/s)		
x, y	Cartesian coordinates	<i>Subscripts</i>	
X, Y	dimensionless Cartesian coordinates	∞	ambient condition
W	cavity width (m)	i	initial condition and index for a number of points in x direction
		j	index for a number of points y -direction
<i>Greek letters</i>			
κ	permeability of porous medium (m ²)		
α	thermal diffusivity (m ² /s)		

Rayleigh number play an important role on mixed convection flow inside a square cavity filled with a fluid-saturated porous media. Nithiarasu et al. [10] examined effects of applied heat transfer coefficient on the cold wall of the cavity upon flow and heat transfer inside a porous medium. The differences between the Darcy and non-Darcy flow regime are clearly investigated for different Darcy, Rayleigh and Biot numbers and aspect ratio. Variations in Darcy, Rayleigh and Biot numbers and aspect ratio significantly affect natural flow convective pattern. Recently, Al-Amiri [11] performed numerical studies of momentum and energy transfer in a lid-driven cavity filled with a saturated porous medium. In this study, the force convection is induced by sliding the top constant-temperature wall. It was found that the increase in Darcy number induces flow activities causing an increase in the fraction of energy transport by means of convection. With similar description of the domain configuration, Khanafer and Vafai [12] extended the investigation to mass transport in the medium. The buoyancy effects that create the flow are induced by both temperature and concentration gradients. It was concluded that the influences of the Darcy number, Lewis number and buoyancy ratio on thermal and flow behaviors were significant. Furthermore, the state of art regarding porous medium models has been summarized in the recently published books [13–15].

Previous investigations have merely focused on momentum and energy transfer in cavity filled with a saturated porous medium subjected to prescribed temperature and prescribed wall heat flux conditions. However, only a very limited amount of numerical and experimental work on momentum and energy transfer in a cavity filled with a sat-

urated porous medium subjected to heat transfer coefficient boundary condition at the exposed portion of the top wall has been reported. The case, in which the top wall is partially exposed, is considered in our study. In this case, the heating pattern is similar to the heating phenomenon occurring in a microwave heating of water layer in which the microwave energy transfers only partially through the top surface for a particular mode of microwave field [16]. It is found in the present study that the two symmetrical vortices are developed during the early stages of heating process. This suggests the presence of heat convection mechanism due to fluid motion in the transient condition. This distinct phenomenon is different from the case of fully heated top wall to which constant temperature was prescribed in that in this case the heat transfer from the top to bottom surface is exclusively by conduction.

In the present study, the detailed parametric study has been carried out for transient natural convective flow in a fluid-saturated porous medium filled in a square cavity. The top surface is partially open to the ambient, allowing the surface temperature to vary, depending on the influence of convection heat transfer mechanism. The influences of associated parameters such as heat transfer coefficient, Rayleigh number and Darcy number on the flow and thermal configurations were examined.

2. Problem description

The computational domain, depicted in Fig. 1 is a rectangular cavity of size $W \times H$ filled with a fluid-saturated porous medium. Aspect ratio of unity ($A = 1$) is used in the present study. The domain boundary is insulated except

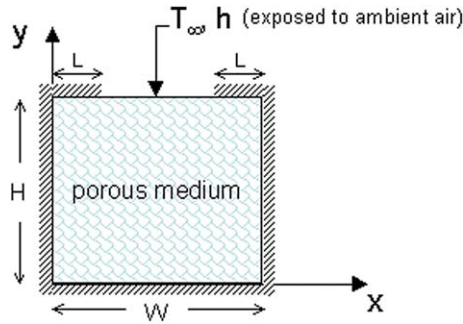


Fig. 1. Schematic representation of the computational domain.

the top wall, which is partially exposed to an ambient air. The initial and boundary conditions corresponding to the problem are of the following forms:

$$u = v = 0, \quad T = T_i \quad \text{for } t = 0, \tag{1}$$

$$u = v = 0 \quad \text{at } x = 0, W \quad 0 \leq y \leq H, \tag{2}$$

$$u = v = 0 \quad \text{at } y = 0, H \quad 0 \leq x \leq W,$$

$$\frac{\partial T}{\partial x} = 0 \quad \text{at } x = 0, W \quad 0 \leq y \leq H,$$

$$\frac{\partial T}{\partial y} = 0 \quad \text{at } y = 0 \quad 0 \leq x \leq W,$$

$$\frac{\partial T}{\partial y} = 0 \quad \text{at } y = H \quad 0 \leq x \leq L \quad \text{and} \quad W - L \leq x \leq W. \tag{3}$$

The boundary condition at the exposed portion of the top wall is defined as

$$-k \frac{\partial T}{\partial y} = h[T - T_\infty] \quad \text{at } y = H \quad L \leq x \leq W - L, \tag{4}$$

where k and h are effective thermal conductivity and convection heat transfer coefficient. ϵ and ν denotes porosity of porous medium and fluid viscosity, respectively. This type of condition corresponds to the existence of convective heat transfer at the surface and is obtained from the surface energy balance.

The porous medium is assumed to be homogeneous and thermally isotropic and saturated with a fluid that is local thermodynamic equilibrium with the solid matrix. The fluid flow is unsteady, laminar and incompressible. The pressure work and viscous dissipation are all assumed negligible. The thermophysical properties of the porous medium are taken to be constant. However, the Boussinesq approximation takes into account of the effect of density variation on the buoyancy force. Furthermore, the solid matrix is made of spherical particles, while the porosity and permeability of the medium are assumed to be uniform throughout the rectangular cavity. Using standard symbols, the governing equations describing the heat transfer phenomenon are given by

$$\frac{\partial u}{\partial x} + \frac{\partial v}{\partial y} = 0, \tag{5}$$

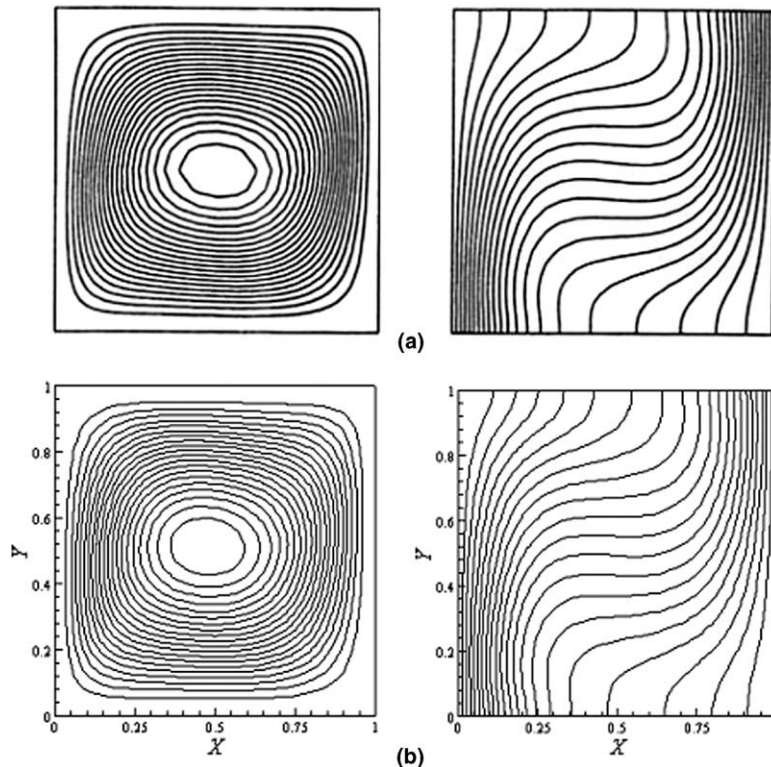


Fig. 2. Test results for validation purpose: (a) previously published results [19] and (b) present numerical simulation.

$$\frac{1}{\varepsilon} \frac{\partial u}{\partial t} + \frac{u}{\varepsilon^2} \frac{\partial u}{\partial x} + \frac{v}{\varepsilon^2} \frac{\partial u}{\partial y} = -\frac{1}{\rho_f} \frac{\partial P}{\partial x} + \frac{v}{\varepsilon} \left(\frac{\partial^2 u}{\partial x^2} + \frac{\partial^2 u}{\partial y^2} \right) - \frac{\mu u}{\rho_f \kappa}, \quad (6)$$

$$\frac{1}{\varepsilon} \frac{\partial v}{\partial t} + \frac{u}{\varepsilon^2} \frac{\partial v}{\partial x} + \frac{v}{\varepsilon^2} \frac{\partial v}{\partial y} = -\frac{1}{\rho_f} \frac{\partial P}{\partial y} + \frac{v}{\varepsilon} \left(\frac{\partial^2 v}{\partial x^2} + \frac{\partial^2 v}{\partial y^2} \right) + g\beta(T - T_\infty) - \frac{\mu v}{\rho_f \kappa}, \quad (7)$$

$$\sigma \frac{\partial T}{\partial t} + u \frac{\partial T}{\partial x} + v \frac{\partial T}{\partial y} = \alpha \left(\frac{\partial^2 T}{\partial x^2} + \frac{\partial^2 T}{\partial y^2} \right), \quad (8)$$

$$\sigma = \frac{[\varepsilon(\rho c_p)_f + (1 - \varepsilon)(\rho c_p)_s]}{(\rho c_p)_f}, \quad (9)$$

where κ is medium permeability, β is thermal expansion coefficient, α is effective thermal diffusivity of the porous

medium, μ and ν are viscosity and kinematic viscosity of the fluid respectively. In the present study, the heat capacity ratio σ is taken to be unity since the thermal properties of the solid matrix and the fluid are assumed identical. The momentum equation consists of the Brinkmann term, which accounts for viscous effects due to the presence of solid body [17]. This form of momentum equation is known as Brinkmann-extended Darcy model. Lauriat and Prasad [18] employed the Brinkmann-extended Darcy formulation to investigate the buoyancy effects on natural convection in a vertical enclosure. Although the viscous boundary layer in the porous medium is very thin for most engineering applications, inclusion of this term is essential for heat transfer calculations [11]. However, the inertial effect was neglected, as the flow was relatively low.

The variables are transformed into the dimensionless quantities defined as,

Table 1
Comparison of the results obtained in the present study with those of Aydin [14]

	Present work	Published work [14]	Difference (%)
ψ_{\max}	5.070	5.087	0.33
U_{\max}	16.300	16.225	0.46
V_{\max}	19.730	19.645	0.43

Table 2
Comparison of the results obtained in the present study with those of Nithiarasu et al. [8]

	Present work	Published work [8]	Difference (%)
ψ_{\max}	2.53	2.56	1.17
V_{\max}	9.49	9.34	1.60

($Da = 0.01$, $Ra = 10^3$, porosity = 0.6).

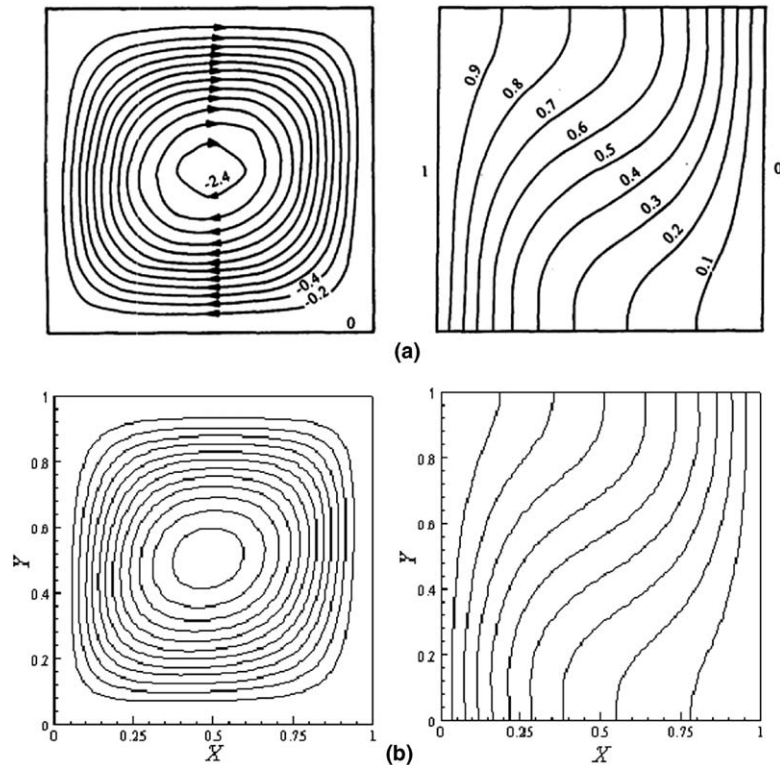


Fig. 3. Test results for validation purpose: (a) Nithiarasu et al. [8]: Non-Darcian model (including inertial and boundary effect) and (b) present simulation: Brinkman-extended Darcy model, which accounts for viscous effects due to the solid boundary.

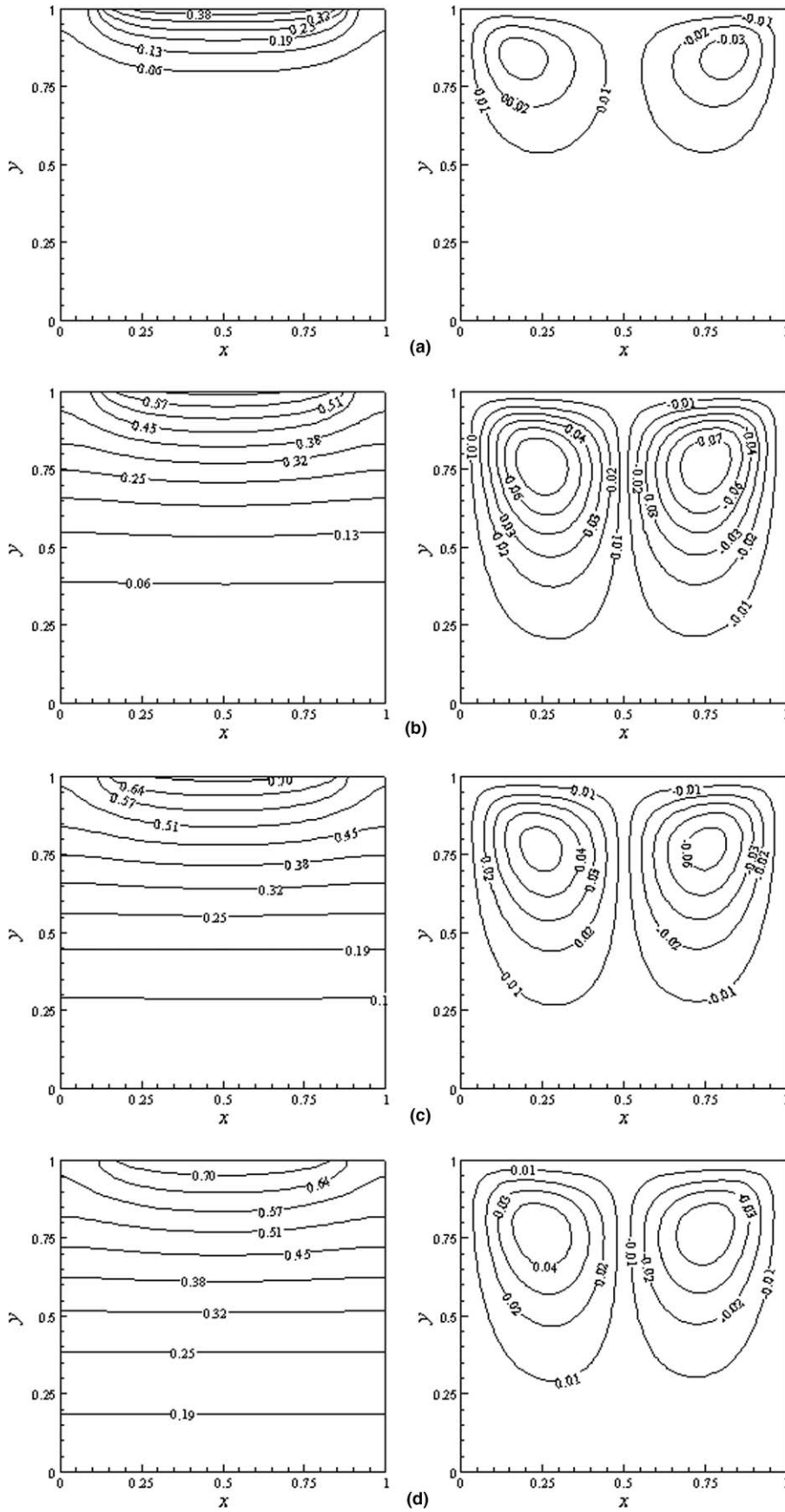


Fig. 4. Sequential files for contours of temperature and streamlines at times $\tau = 0.0125, 0.09, 0.1675,$ and 0.2475 . ($Ra = 10^4, Da = 0.01, Pr = 1.0, \varepsilon = 0.8,$ and $h = 100 \text{ W/m}^2 \text{ K}$).

$$\begin{aligned}
 X = \frac{x}{H}, \quad Y = \frac{y}{H}, \quad \tau = \frac{t\alpha}{H^2}, \quad U = \frac{uH}{\alpha}, \\
 V = \frac{vH}{\alpha}, \quad \zeta = \frac{\omega H^2}{\alpha}, \quad \Psi = \frac{\psi}{\alpha}, \quad \theta = \frac{T - T_i}{T_\infty - T_i}, \quad (10)
 \end{aligned}$$

where ω and ψ represent dimensional vorticity and stream function, respectively. Symbol α denotes thermal diffusivity. The initial temperature and ambient temperature are given by T_i and T_∞ . Thus the dimensionless form of the governing equations can be written as

$$\frac{\partial^2 \psi}{\partial X^2} + \frac{\partial^2 \psi}{\partial Y^2} = -\zeta, \quad (11)$$

$$\begin{aligned}
 \varepsilon \frac{\partial \zeta}{\partial \tau} + U \frac{\partial \zeta}{\partial X} + V \frac{\partial \zeta}{\partial Y} = \varepsilon Pr \left(\frac{\partial^2 \zeta}{\partial X^2} + \frac{\partial^2 \zeta}{\partial Y^2} \right) \\
 + \varepsilon^2 Ra Pr \left(\frac{\partial \theta}{\partial X} \right) - \frac{\varepsilon^2 Pr}{Da} \zeta, \quad (12)
 \end{aligned}$$

$$\sigma \frac{\partial \theta}{\partial \tau} + U \frac{\partial \theta}{\partial X} + V \frac{\partial \theta}{\partial Y} = \alpha \left(\frac{\partial^2 \theta}{\partial X^2} + \frac{\partial^2 \theta}{\partial Y^2} \right), \quad (13)$$

where the Darcy number, Da is defined as κ/H^2 , and $Pr = \nu/\alpha$ is a prandtl number. The Rayleigh number Ra , which gives the relative magnitude of buoyancy and viscous forces is defined as $Ra = g\beta(T_i - T_\infty)H^3/(\nu\alpha)$.

$Pr = \nu/\alpha$ is the Prantl number, where $\alpha = k_c/(\rho c_p)_f$ is the thermal diffusivity.

3. Numerical procedure

The thermal properties of the porous medium are taken to be constant. Specific heat ratio of unity is assumed. The effective thermal conductivity of the porous medium considered is 10 W/m K.

In the present study, the iterative finite difference method is used to solve the transient dimensionless governing equations (Eqs. (11)–(13)) subject to their corresponding initial and boundary conditions given in Eqs. (1)–(4). Approximation of convective terms is based on an upwind finite differencing scheme, which correctly represent the directional influence of a disturbance. A uniform grid resolution of 61×61 was found to be sufficient for all smooth computations and computational time required in achieving steady-state conditions. Finer grids did not provide a noticeable change in the computed results. The finite difference form of boundary condition at the open part of the top surface is systematically derived, based on energy conservation principle. The boundary values of dimensionless temperature of a node i, j $\theta_{i,j}$ are expressed as

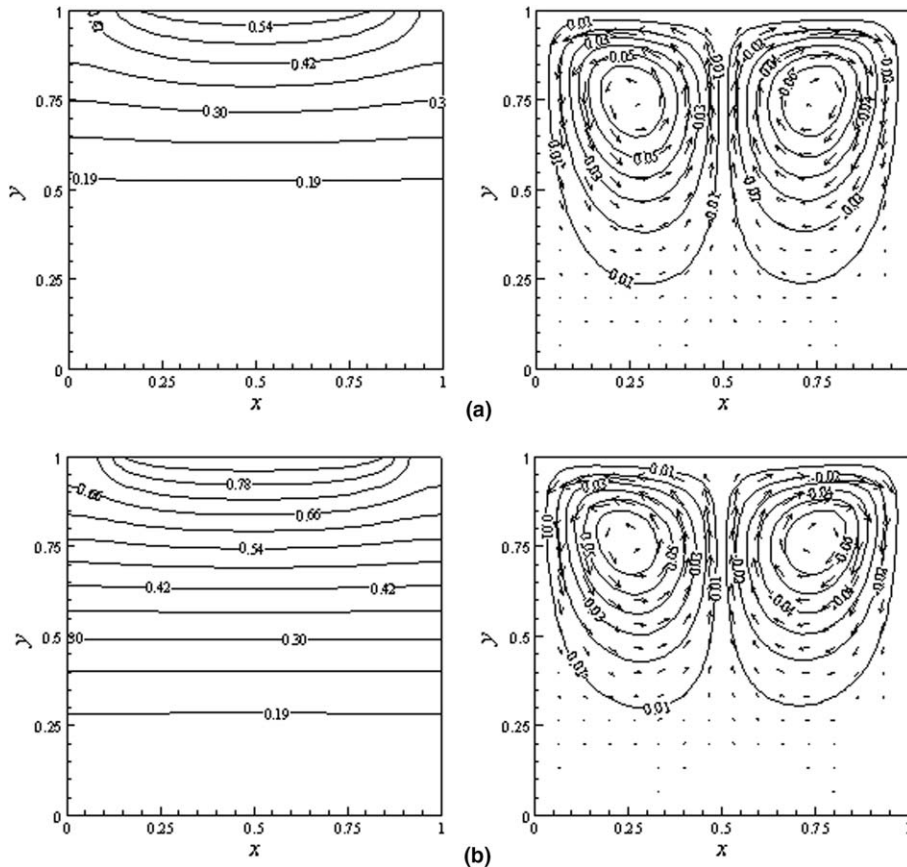


Fig. 5. Contours of temperature and streamlines: (a) $h = 60 \text{ W/m}^2 \text{ K}$ and (b) $h = 300 \text{ W/m}^2 \text{ K}$. ($Ra = 10^4$, $Da = 0.1$, $Pr = 1.0$, and $\varepsilon = 0.8$).

$$\theta_{ij} = \frac{2\theta_{ij-1} + \theta_{i-1j} + \theta_{i+1j} + 2\frac{h\Delta y}{k}}{2(\frac{h}{k}\Delta Y + 2)} \quad (14)$$

It can be noticed that Eq. (14) is independent of T_∞ as it has been eliminated during the derivation. Thus the solutions can be obtained regardless of a value of T_∞ .

4. Results and discussion

In order to verify the accuracy of the present numerical study, the present numerical model was validated against the results obtained by Aydin [19] for a free convection flow in a cavity, with side-heated isothermal wall, filled with pure

air ($Pr = 0.7$) for Rayleigh number of 10^4 . It was found that the solutions have good agreement with the previously published work. The results of the selected test case are illustrated in Fig. 2 for streamlines and temperature contour lines. Table 1 clearly shows a good agreement of the maximum value of the stream function and the maximum values of the horizontal and vertical velocity components between the present solution and that of Aydin. Also, the results from the present numerical model were compared with the solution of Nithiarasu et al. [8] in the presence of porous medium for additional source of confidence, as shown in Fig. 3. The values of $Ra = 10^4$, $Da = 0.01$ and $\varepsilon = 0.6$ were chosen. Table 2 clearly shows a good agreement of the

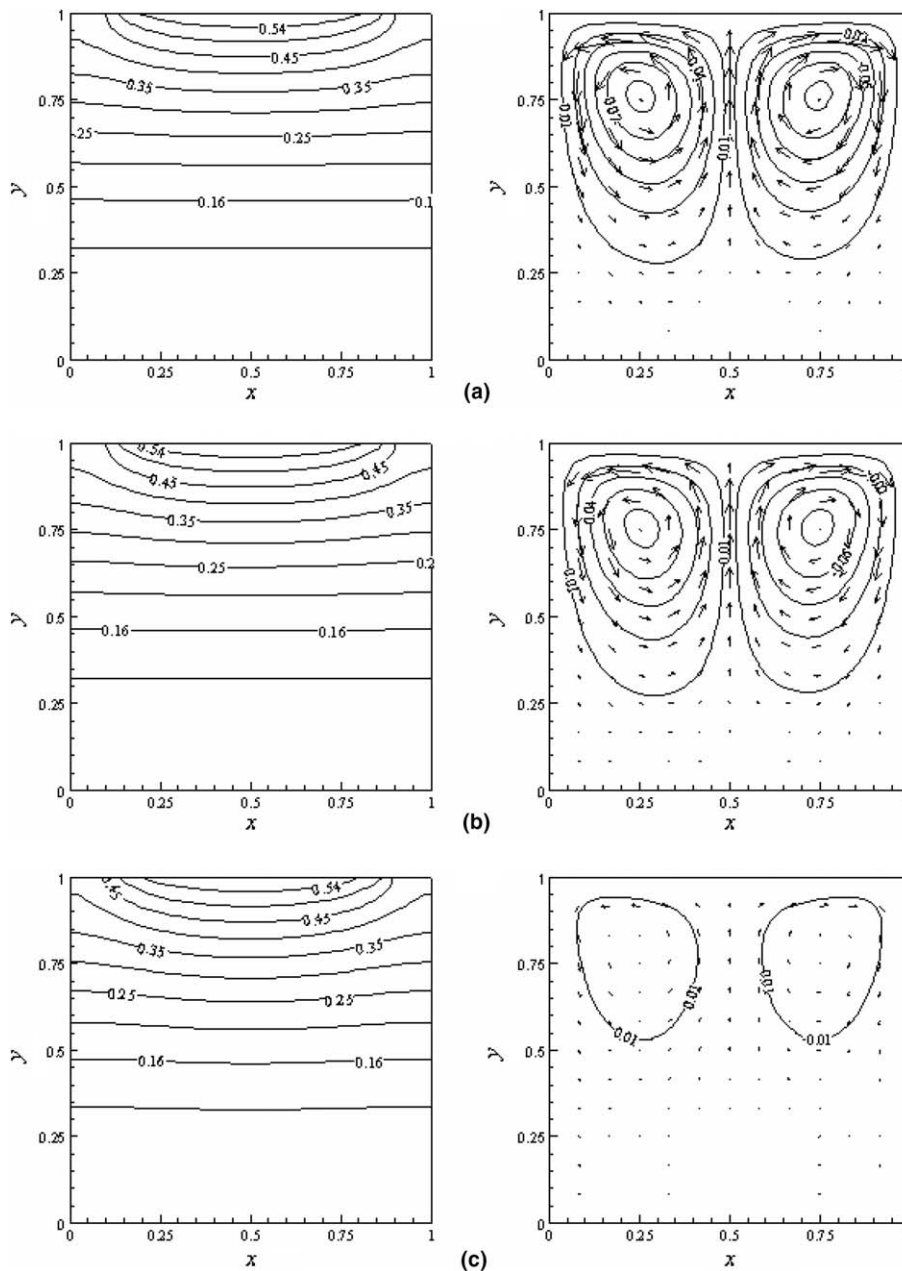


Fig. 6. Contours of temperature and streamlines: (a) $Da = \text{infinity}$, (b) $Da = 0.1$, (c) $Da = 0.001$. ($Ra = 10^4$, $h = 60 \text{ W/m}^2 \text{ K}$, $Pr = 1.0$, and $\varepsilon = 0.8$).

maximum values of the stream function and vertical velocity component between the present solution and that of Nithiarasu et al [8]. All of these favorable comparisons lend confidence in the accuracy of the present numerical model.

The following discussions include the numerical results from the present study. Initial values of θ for an entire domain are set 1, based on Eq. (14) since the ambient temperature is higher than temperature of the medium in cavity. The investigations were conducted for a range of controlling parameters, which are Darcy number (Da) Rayleigh number (Ra) and convective heat transfer coefficient (h). The porosity ε of 0.8 and unity aspect ratio ($A = 1$) were considered throughout in the present study. In order to assess global effects of these parameters, the streamlines and isotherm distributions inside the entire cavity are presented. All the figures have the same range of contour levels to facilitate direct comparisons.

The resulting computational fields were extracted at the time adequately long to ensure sufficient energy transferred throughout the domain. Fig. 4 displays instantaneous images of the contour plots during the thermal and flow evolution. The Darcy number of 0.01, $Pr = 1.0$, $h = 60 \text{ W/m}^2 \text{ K}$, and $\varepsilon = 0.8$ are considered. The two columns represent temperature and stream function. With the same contour levels, comparisons can be observed directly. The four snapshots from top to bottom in each column are results taken at the dimensionless times $\tau = 0.0125, 0.09, 0.1675$, and 0.2475 with the time interval. The vertical temperature stratification is observed. The streamline contours exhibit circulation patterns, which are characterized by the two symmetrical vortices. The fluid flows as it is driven by the effect of buoyancy. This effect is distributed from the top wall of cavity where the fluid is heated through the partially open area. This indicates the non-uniform temperature at the top surface, leading to an unstable condition. Thus the buoyancy effect is associated with the lateral temperature gradient at locations near the top surface. Heated portions of the fluid become lighter than the rest of fluid, and are expanded laterally away from the center to the sides then flow down along the two vertical walls, leading to the clockwise and counter-clockwise flow circulations. These results suggest that the buoyancy forces are able to overcome the retarding influence of viscous forces. An increase in strength of the vortices develops fast during early simulation times, and its maximum magnitude reaches 0.1 at $\tau = 0.0475$. After this time, the vortices are slowly weakened. Similarly, temperature distribution progressively evolves relatively fast in the early times. After the time $\tau = 0.07$, slow evolution is observed. This result corresponds to the decrease in strength of flow circulations. In the remaining area, the fluid is nearly stagnant suggesting that conduction is dominant due to minimal flow activities. This is because the viscous effects are large.

This distinct phenomenon is different from the case of fully heated top wall to which constant temperature was prescribed in that in this case the heat transfer from the top to bottom surface is exclusively by pure conduction.

Fig. 5 illustrates how the convective heat transfer coefficient influences thermal and flow behaviors, while other parameters $Da = 0.1$, $Pr = 1.0$, and $\varepsilon = 0.8$ are fixed. The variable values of h chosen are 60 and $300 \text{ W/m}^2 \text{ K}$, which may represent a typical free and forced convection, respectively. In all the figures henceforth, directions and magnitudes of the arrows indicate the direction as well as strength of the flows respectively. It is seen on the left column in Fig. 5 that the temperature gradients are steep at the top area near the exposed convective surface and gradually decreases toward the bottom of the domain. In the remaining area of the cavity, the temperature gradients are small and this implies that the temperature differences are very small in the bottom region of the cavity where viscous effects are strong. It can be observed on the right-column plots, which presents streamline contours that the change in h does not contribute a significant modification to the temperature contours. However, an increase in h expands temperature distribution area due to the more energy that is carried away from the location of convection surface condition toward the bottom. Moreover, higher value of h increases maximum temperature resulting in wider temperature range in the domain.

Effects of the Darcy number on the fluid flow and temperature inside the rectangular cavity are depicted in Fig. 6. The contour of isotherms and streamlines are plotted for different Darcy numbers while ε , Pr and h are kept at 0.8, 1.0 and $60 \text{ W/m}^2 \text{ K}$ respectively. The Darcy number, which is directly proportional to the permeability of the porous medium, was set to 0.001 and 0.1. The case in which the porous medium is absent corresponds to infinite Darcy number. The presence of a porous medium within rectangular enclosure results in a force opposite to the flow direction which tends to resist the flow which corresponds to suppress in the thermal currents of the flow as compared to a medium with no porous (infinite Darcy number). It is evident that the increase in Da enhances the streamline

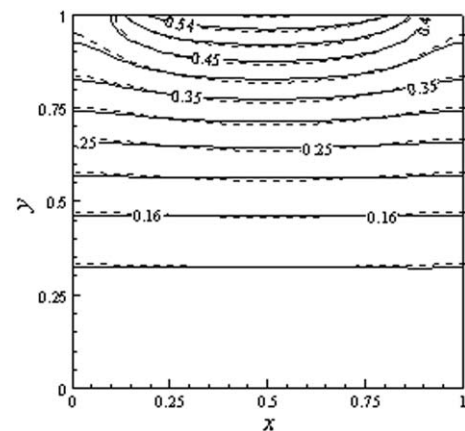


Fig. 7. Temperature distribution contours within a medium in the absent of porous (solid line) overlaid by the temperature distribution contours in a porous medium with Da of 0.001 (dash line). Data is taken from that of Fig. 6.

intensities thereby assisting downward flow penetration, which causes the streamline lines, i.e., two symmetrical vortices to stretch further away from the top surface. This results in expanding the region for which the convection significantly influences an overall heat transfer process. On the other hand, as the Darcy number decreases, the flow circulations as well as thermal penetration are progressively inhibited due to the reduced permeability of the medium except at the region close to the location of convection surface condition where the flow motions are relatively strong. Furthermore, Fig. 6c indicates that as Darcy number approaches zero, the convective heat transfer mechanism is almost suppressed, while the heat transfer by means of conduction plays an important role in heat

transfer. The left column of Fig. 6 shows comparison of temperature in which the contours of different Darcy numbers appear roughly similar.

To gain further insight into the effects of the Darcy number on the thermally stratified layer, temperature contours for pure fluid are overlaid with that for porous fluid with Da of 0.001. The results are given in Fig. 7. It is noticed that temperature stratification layers, near the vertical symmetry line in the case of Da 0.001, move further downward relative to those for pure fluid. This observed incident results from a stronger flow in the upward direction in the central region for the pure medium. The upward flows inhibit the thermal propagation. In contrast, in the areas away from the vertical center line, the downward flows

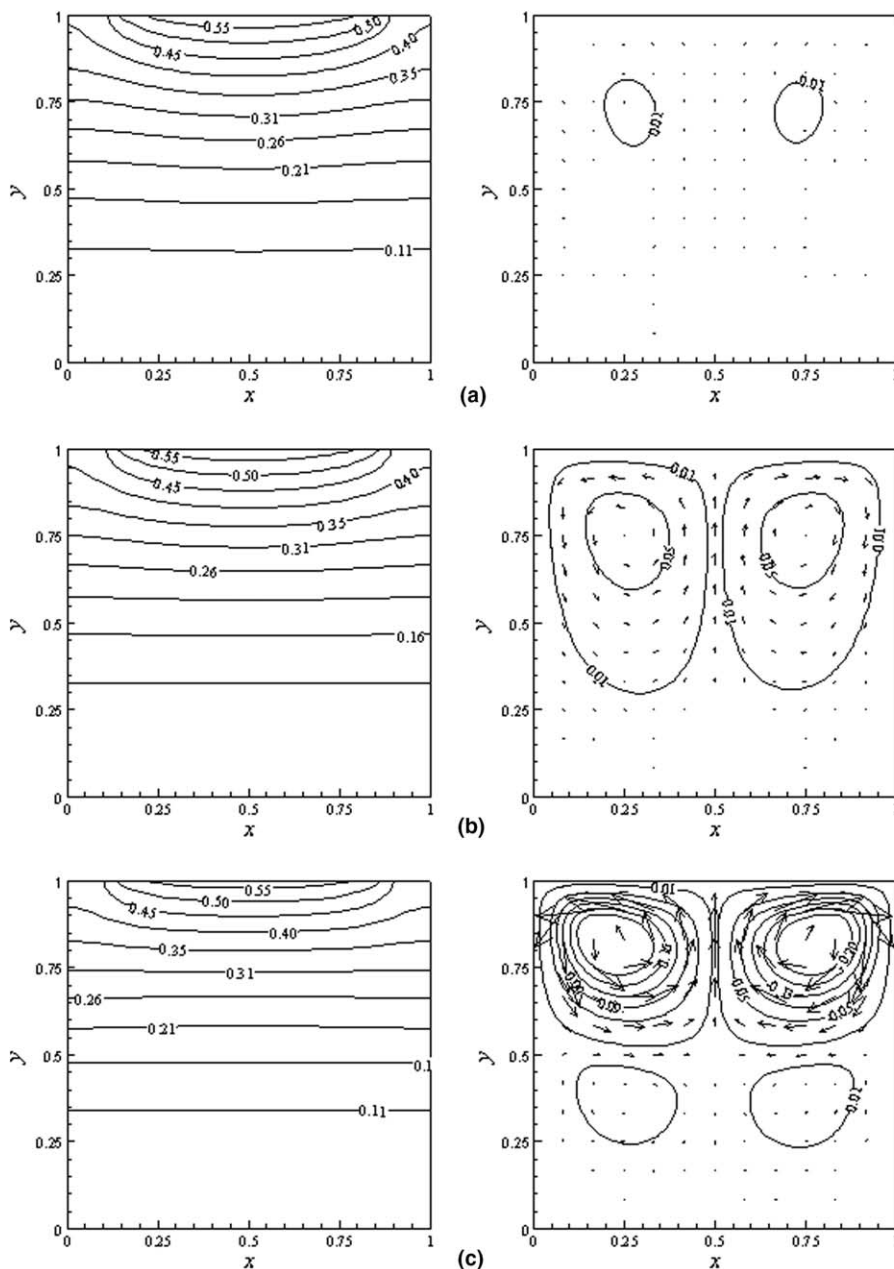


Fig. 8. Contours of temperature and streamlines: (a) $Ra = 10^3$, (b) $Ra = 10^4$ and (c) $Ra = 10^5$. ($Da = 0.1$, $h = 60 \text{ W/m}^2 \text{ K}$, $Pr = 1.0$, and $\varepsilon = 0.8$).

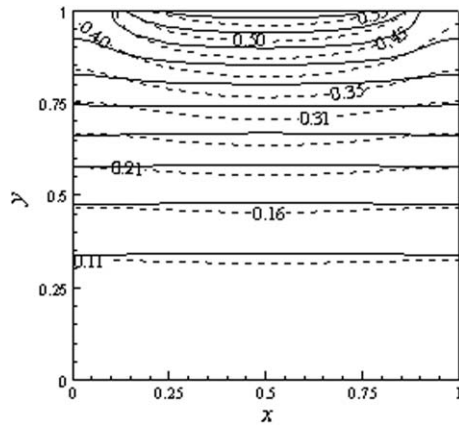


Fig. 9. Temperature distribution contours within a porous medium with $Ra = 10^3$ (dash line) overlaid by the temperature distribution contours in a porous medium with $Ra = 10^5$ (solid line). Data is taken from that of Fig. 8.

assist heat to be transferred towards the bottom of the enclosure.

Fig. 8 shows the isotherms and streamlines obtained for various Rayleigh numbers ($Ra = 10^3$, 10^4 and 10^5) whereas the Darcy number of 0.1, porosity of 0.8, and h of $60 \text{ W/m}^2 \text{ K}$ are fixed. The Rayleigh number provides the ratio of buoyancy forces to change in viscous forces. As Rayleigh number increases, the buoyancy-driven circulations inside the enclosure become stronger as seen from greater magnitudes of stream function. For the large value of Ra ($Ra = 10^5$), there appears a pair of secondary weak circulations in the bottom region of the enclosure. The two vigorous vortices are confined to the upper domain, where convection is a dominant mode of heat transfer.

Although the profiles of temperature contour are qualitative similar, Fig. 9 displays overlaid contours for the two cases which are of $Ra = 10^3$ and $Ra = 10^5$. It is evident in the case of $Ra = 10^3$ that temperature contour lines penetrate faster relative to the low Ra case at the central locations around vertical symmetric line, but they move slower in the regions near the vertical walls. The results are consistent with the thermal behaviors observed in Fig. 7 for the same reasoning, which confirm how a flow direction impacts the convection heat transfer. Therefore it can be concluded to an interesting note that not only an intensity of a flow, but also the direction of the fluid flow locally affects the heat convection process.

5. Conclusions

Numerical simulations of natural convection flow through a fluid-saturated porous medium in a rectangular cavity due to top surface convection were performed. Transient effects of associated controlling parameters were examined. The two-dimensional flow is characterized mainly by two symmetrical eddies that are initiated by the presence of buoyancy effect. The buoyancy effect is associated with the lateral temperature gradient at loca-

tions near the top surface. As the convection heat transfer coefficient increases, the temperature stratification penetrates deeper toward the bottom wall, and temperature range within the domain is extended. Small values of Darcy number hinder the flow circulations. Therefore the heat transfer by convection is considerably suppressed. Large values of Rayleigh number increase streamline intensities, thus enhancing the downward flow penetration. Therefore enlarges the region where convection mode is significant. Moreover, the flow in the direction of heat transfer is found to enhance the rate of convection whereas the flow in the opposed direction retards the heat rate. In our future study, effects of internal heat generation due to microwave energy on heat transfer processes in fluid-saturated porous medium will be considered.

Acknowledgement

This research was financially supported by the Thailand Research Fund (TRF).

References

- [1] T.L. Bergman, F.P. Incropera, R. Viskanta, Correlation of mixed layers growth in double-diffusive, salt-stratified system heated from below, *J. Heat Transfer* 108 (1986) 206–211.
- [2] J. Imberger, P.F. Hamblin, Dynamics of lakes, reservoirs, and cooling ponds, *A. Rev. Fluid Mech.* 14 (1982) 153–187.
- [3] M.A. Stanish, G.S. Schager, F. Kayihan, A mathematical model of drying for hygroscopic porous media, *AIChE J.* 32 (1986) 1301–1311.
- [4] P. Ratanadecho, K. Aoki, M. Akahori, A numerical and experimental investigation of the modeling of microwave drying using a rectangular wave guide, *J. Drying Technol.* 19 (9) (2001) 2209–2234.
- [5] P. Ratanadecho, K. Aoki, M. Akahori, Influence of irradiation time, particle sizes and initial moisture content during microwave drying of multi-layered capillary porous materials, *ASME J. Heat Transfer* 124 (1) (2002) 151–161.
- [6] P. Cheng, Heat transfer in geothermal systems, *Adv. Heat Transfer* 4 (1978) 1–105.
- [7] P.H. Oosthuizen, H. Patrick, Natural Convection in an Inclined Square Enclosure Partly Filled with a Porous Medium and with a Partially Heated Wall, *HTD 302*, American Society of Mechanical Engineers, Heat Transfer Division, (Publication), 1995, pp. 29–42.
- [8] P. Nithiarasu, K.N. Seetharamu, T. Sundararajan, Natural convective heat transfer in a fluid saturated variable porosity medium, *Int. J. Heat Mass Transfer* 40 (16) (1997) 3955–3967.
- [9] K.M. Khanafer, A.J. Chamkha, Mixed convection flow in a lid-driven enclosure filled with a fluid-saturated porous medium, *Int. J. Heat Mass Transfer* 42 (13) (1998) 2465–2481.
- [10] P. Nithiarasu, K.N. Seetharamu, T. Sundararajan, Numerical investigation of buoyancy driven flow in a fluid saturated non-Darcian porous medium, *Int. J. Heat Mass Transfer* 42 (7) (1998) 1205–1215.
- [11] A.M. Al-Amiri, Analysis of momentum and energy transfer in a lid-driven cavity filled with a porous medium, *Int. J. Heat Mass Transfer* 43 (2000) 3513–3527.
- [12] K. Khanafer, K. Vafai, Double-diffusive mixed convection in a lid-driven enclosure filled with a fluid-saturated porous medium, *Numer. Heat Transfer, Part A* 42 (2002) 465–486.
- [13] D.A. Nield, A. Bejan, *Convection in Porous Media*, Springer, New York, 1999.
- [14] K. Vafai, *Handbook of Porous Media*, Marcel Dekker, New York, 2000.

- [15] I. Pop, D.B. Ingham, *Convective Heat Transfer, Mathematical and Computational Modeling of Viscous Fluids and Porous Media*, Pergamon, Oxford, 2001.
- [16] P. Ratanadecho, K. Aoki, M. Akahori, A numerical and experimental investigation of the modeling of microwave heating for liquid layers using a rectangular wave guide (effects of natural convection and dielectric properties), *Appl. Math. Modelling* 26 (2002) 449–472.
- [17] H.C. Brinkmann, On the permeability of media consisting of closely packed porous particles, *Appl. Sci. Res.* 1 (1947) 81–86.
- [18] G. Lauriat, V. Prasad, Natural convection in a vertical porous cavity: a numerical study for Brinkmann-extended Darcy formulation, *Trans. ASME J. Heat Transfer* 109 (1987) 295–320.
- [19] O. Aydin, Determination of optimum air-layer thickness in double-pane windows, *Energy Buildings* 32 (2000) 303–308.